Loss of p53 and Acquisition of Angiogenic MicroRNA Profile Are Insufficient to Facilitate Progression of Bladder Urothelial Carcinoma *in Situ* to Invasive Carcinoma*⒮

Francisco Ayala de la Peña[‡1], **Keizo Kanasaki**[‡], **Megumi Kanasaki**[‡], **Neelima Tangirala**[‡], **Genta Maeda**[‡], **and Raghu Kalluri**[‡§¶2]

From the ‡Division of Matrix Biology, Department of Medicine, Beth Israel Deaconess Medical Center and Harvard Medical School, Boston, Massachusetts 02215, the §Harvard-MIT Division of Health Sciences and Technology, Harvard Medical School, Boston, Massachusetts 02215, and the ¶Department of Biological Chemistry and Molecular Pharmacology, Harvard Medical School, Boston, Massachusetts 02215

Activation of oncogenes or inactivation of tumor suppressors in urothelium is considered critical for development of urothelial cancer. Here we report cloning of the urothelium-specific promoter uroplakin-II (UPK II) and generation of transgenic mice in which expression of SV40 large T antigen is driven by UPK II promoter. Inactivation of tumor suppressor p53 and pRb in urothelium by SV40 T antigen resulted in urothelial carcinoma, resembling human high-grade carcinoma *in situ*. Specific deletion of p53 in urothelial cells using the newly generated UPK II-Cre mice results in normal bladders without any evidence of cancer. The high-grade carcinoma *in situ* in the UPK II-SV40 mice is associated with significant activation of angiogenic signals consisting of hypoxia-inducible factor-1α (HIF-1α) and VEGF and a down-regulation of thrombospondin-1. Interestingly, such pro-angiogenic activity was not associated with progression to invasive cancer. Analysis of bladder-associated microRNAs in carcinoma *in situ* lesions reveals a pro-angiogenic profile, with specific overexpression of miR-18a and miR-19a and down-regulation of miR-107. A group of microRNAs (miRs) identified as associated with invasive human urothelial cancer remained unchanged in this mouse model. Collectively, our results support the notion that activation of angiogenesis and loss of p53 are not sufficient for progression to invasive cancer. Our studies identify a new mouse model for bladder cancer that can be used to study factors that determine progression to an invasive phenotype of bladder cancer.

Urothelial carcinomas of the bladder are among the most frequent human cancers and account for more than 14,000 deaths annually in the United States (1). Most cases of urothelial cancer are superficial bladder tumors, but around 20% of them are invasive carcinomas that can generate metastasis at the initial presentation or later in the evolution of the disease. Two groups of superficial bladder tumors have been described (2). Low grade papillary neoplasms are the most frequent, with a low potential of transformation into invasive cancer. Conversely, carcinomas *in situ* (CIS)[3] are biologically more aggressive and carry a high probability of turning into an invasive carcinoma. The molecular basis of urothelial bladder cancer is being progressively unveiled, and the generation of transgenic mouse models of bladder cancer obtained through the urothelial expression of oncogenes (SV40) (3) or deletion of tumor suppressor genes remains a viable strategy for unraveling this mechanism. It is acknowledged that there are at least two different pathways driving the malignant transformation of urothelium, each of them corresponding to one of the two types of urothelial tumors. The pathway leading to CIS, which is speculated to involve a loss of function of p53 (4), is particularly important due to its role as precursor of invasive disease. However, p53 deletion does not seem to be sufficient for urothelial tumorigenesis unless there is either a concurrent deletion of pRb (5, 6) or Pten (7) or a concurrent H-ras activation (8).

Bladder urothelial carcinoma *in situ* poses a difficult conundrum in the clinical setting. Its high recurrence rate (90% of cases) and its frequent evolution to invasive disease make it a target for aggressive treatment regimens, such as bladder bacillus Calmette-Guerin therapy or cystectomy as in cases of extensive or persistent disease presentation (9). Angiogenesis is among the biological factors that have been studied as potential predictors of progression to invasive tumors in superficial bladder carcinoma and is considered by some groups as a useful biomarker (10). In this regard, some clinical studies have suggested that elevated microvessel density, an indicator of angiogenic phenotype, is associated with progression of carcinoma *in situ* to invasive cancer, but some other clinical observations did not confirm these results (11, 12). Similar conflicting results have been reported for VEGF levels in urine or plasma (13) or for VEGF and HIF-1α expression in the tumor, which some authors suggest as important for progression to invasive cancer (14–16). Most studies include both CIS and pT1a types of

[3] The abbreviations used are: CIS, carcinoma *in situ*; miR, microRNA; TSP-1, thrombospondin-1; UPK II, uroplakin II.

tumors, thus making their interpretation confounding. Consequently, the emergence of angiogenic phenotype and its relevance for progression toward invasive bladder carcinoma are still controversial and need experimental validation.

The goal of our study was to determine the role of p53 and angiogenic phenotype in the initiation and progression of bladder cancer. SV40 T antigen expression is able to inactivate both p53 and pRb tumor suppression pathways, and its urothelial conditional expression driven by uroplakin II (UPK II) has been previously shown to generate urothelial bladder carcinoma *in situ*, with late muscle invasion and metastasis in a few mice (3). We generated a new transgenic mouse, UPK II-SV40, and observed that the development of high-grade urothelial carcinoma *in situ* was associated with a significant activation of angiogenic signals. This pro-angiogenic phenotype was independent of invasion and associated with specific changes in the profile of microRNAs regulating angiogenesis, without any effect on urothelial expression of invasion-related microRNA (miR). Lastly, loss of p53 alone in the urothelium did not result in initiation of cancer or angiogenic activation, and mice were normal. Collectively, these results suggest that progression to invasive bladder cancer is not solely dependent on angiogenesis, and therefore, the notion that markers of angiogenesis or angiogenesis-related miRs may serve as useful markers to predict invasive bladder cancer needs to be carefully evaluated.

EXPERIMENTAL PROCEDURES

Gene Constructs and Generation of Transgenic Mice—For the specific urothelial expression of SV40 large T antigen, a construct containing the urothelium-specific promoter uroplakin II (3.6 kb) and the SV40 T antigen was designed. First, we cloned mouse UPK II promoter (accession number: EF467361) from bacterial artificial chromosome clone RP24-308H8 with a PCR-based approach. During the cloning process, we found that about 1500 bp of the UPK II promoter region, which was deposited in GenBank™ (accession number U14421), was oppositely inserted between the two SacI restriction enzyme sites (from -1262 to -2805 from exon 1) in UPK II promoter. SV40 early sequence DNA was obtained from the Rip-TAG vector (kindly provided by Dr. Douglas Hanahan). The chimeric gene containing (5′ to 3′) the UPK II promoter (3.6 kb), the SV40 T antigen sequence (3.0 kb), and a 250-bp poly(A) signal was excised from the vector with EcoRI and BamHI digestion and purified with the Illustra GFX PCR DNA and gel band purification kit (GE Healthcare). Additionally, we also generated a transgenic mouse that expresses the Cre recombinase enzyme in bladder uroepithelium by utilizing the same UPK II promoter. Microinjection of the purified constructs in the pronuclei of fertilized eggs from C57/BL mice was performed for generation of transgenic mice (UPK II-SV40 and UPK II-Cre) at the Beth Israel Deaconess Medical Center transgenic facility.

For specific urothelial knock-out of p53, the UPK II-Cre mouse strain described before was interbred to p53 floxed mice (National Institutes of Health, NCI, Mouse Repository) in which LoxP sites have been inserted in introns 1 and 10 of the p53 gene. To confirm urothelium-restricted expression of UPK II, a reporter strain was generated by interbreeding the UPK II-Cre with Rosa-R26R-YFP floxed mice (17).

Genotyping and Animal Experiments—Genotyping of transgenic mice was determined by PCR in genomic DNA isolated from mice tails. The term "controls" refers to littermates of mice with a negative UPK II-SV40, UPK II-Cre;p53 f/f, or UPK II-Cre;YFP genotype. Mice were sacrificed at different time points, and bladders were obtained, weighted, and processed for histological analysis and molecular biology techniques. Thirty minutes before sacrifice, pimonidazole (Hypoxyprobe™-1, HPI Inc.) was intraperitoneally administered at a dose of 60 mg/kg. Mice were maintained at the Beth Israel Deaconess Medical Center animal facility under standard conditions. All animal studies were reviewed and approved by the Institutional Animal Care and Use Committee of Beth Israel Deaconess Medical Center.

Histological Techniques—Paraformaldehyde-fixed, paraffin-embedded 5-μm sections were treated with 10 mM citrate buffer for antigen retrieval, and standard immunohistochemical techniques were applied. The following primary antibodies and dilutions were used: anti-SV40 T antigen (1:50; Santa Cruz Biotechnology), anti-VEGF Ab-1 (10 μg/ml; Thermo Fisher Scientific), anti-HIF-1α (1:50; Santa Cruz Biotechnology), anti-Glut-1 (1:50; Abcam), anti-p53 (1:50; Santa Cruz Biotechnology), and anti-CD34 (1:50; Abcam). Biotinylated secondary antibodies (1:200) and VECTASTAIN ABC kit were used according to the manufacturer's instructions (Vector Laboratories). For hypoxia staining, the Hypoxyprobe™-1 Kit (HPI, Inc.) was used according to the manufacturer's instructions (primary antibody: 1:50 dilution).

For immunofluorescence, 5-μm frozen sections were fixed in 100% acetone at -20 °C for 10 min. Primary antibodies were anti-CD31 (1:50; BD Biosciences Pharmingen), anti-CD34 (1:50; Abcam), anti-VEGF Ab-1 (10 μg/ml; Thermo Fisher Scientific), and anti-NG2 (1:100; Santa Cruz Biotechnology). Sections were subsequently labeled with fluorescein- or rhodamine-conjugated secondary antibodies (Jackson ImmunoResearch Laboratories), and DAPI was used for nuclear counterstaining.

For blood vessel evaluation, a sufficient number of sections to cover the whole area of bladder stroma and urothelium were analyzed at 200×, and the relative area of CD31 staining was quantified with the ImageJ software (National Institutes of Health, Bethesda, MD). For evaluation of pericyte coverage, the proportion of CD31 vessels with perivascular NG2 staining was calculated.

SDS-PAGE and Western Blot Studies—Samples (purified protein from whole bladder) were denatured with SDS sample buffer. Primary antibodies were anti-VEGF (1:500; Oncogene), anti-SV40 (1:100; Santa Cruz Biotechnology), and anti-actin (1:1000; Sigma). After incubation with horseradish peroxidase-conjugated secondary antibodies (Sigma), an enhanced chemiluminescence (ECL) detection system (Pierce Biotechnology) was used.

Real Time RT-PCR and MicroRNA Analysis—Total RNA was isolated from whole bladder tissues using TRIzol® according to the manufacturer's recommendations (Invitrogen). After DNase I treatment (Invitrogen), reverse transcription for mRNA was carried out using the High Capacity cDNA reverse transcription kit (Applied Biosystems). For microRNA studies,

RNA reverse transcription was performed with the ABI TaqMan microRNA reverse transcription kit (Applied Biosystems) using specific stem-loop primers, as described previously (18). Quantification of expression levels of VEGF, thrombospondin-1 (TSP-1), HIF-1α, HIF-1β, Dicer, Drosha, and microRNAs was determined by quantitative real time-PCR using SYBR Green (Applied Biosystems) and an Applied Biosystems 7300 detection system. GAPDH and RNU6B (for microRNA) were used for normalization, and all reactions were run in triplicate. Relative quantification of genes expression was analyzed with the comparative cycle threshold method ($2^{-\Delta\Delta CT}$). Sequences of miR, stem-loop primers, and primers for real time RT-PCR are shown in supplemental Table 1. Other primers for real time RT-PCR are shown in supplemental Table 2.

Statistical Analysis—Data are expressed as mean $\pm$ S.E. Statistical analysis was performed using SPSS version 15.0 (SPSS Inc.). Tests used were non-parametric Mann-Whitney (unpaired, two-tailed), and when appropriate, Student's *t* test. Statistical significance was established as $p \leq 0.05$.

RESULTS

Urothelium-specific Expression of SV40 T Antigen Leads to Development of Bladder Carcinoma in Situ—SV40 T large antigen expression is able to inactivate both p53 and pRb, and its uroplakin II conditional expression has been previously shown to induce the development of bladder CIS (3). We generated a transgenic mouse model in which the newly cloned UPK II promoter drives the expression of the SV40 T antigen (Fig. 1*A*). UPK II-SV40 (+) mice developed bladder urothelial carcinoma *in situ* with a 100% (39/39) penetrance starting from the first week of their life (Fig. 1, *B*–*D* and *F*–*O*). Although both males and females developed bladder carcinomas with similar disease progression kinetics, the bladder weight was higher in males, reflecting a higher tumor burden, as reported previously (19) (Fig. 1*E*). Immunohistochemistry evaluation of paraffin-embedded bladder tissue revealed specific expression of SV40 in urothelial cells from UPK II-SV40 mice (Fig. 1, *P*–*Q*). Bladder transitional carcinomas developed with characteristics of human CIS or high-grade intraurothelial neoplasia (20), exhibiting a flat growth, with large and pleomorphic nuclei and frequent mitoses (Fig. 1*R*). A papillary high-grade pattern appeared later but was infrequent. Although previous reports of similar models showed muscle invasion and occasional metastasis (3, 4), this was an infrequent and late event; accordingly, in our UPK II-SV40 lines, we observed one incidence (1 out of 39) of lamina propria invasion but without muscle involvement or distant metastases (4–6 months). The development of urothelial carcinomas in renal pelvis and ureter followed a similar, but slower, progression (Fig. 1, *S*–*V*).

Analysis of Pro-angiogenic Phenotype of UPK II-SV40 Bladder Carcinoma—The expression of VEGF, the main pro-angiogenic factor in cancer, has been considered a critical factor in SV40-induced tumor progression (21). To analyze the angiogenic pattern in our model of bladder carcinoma *in situ*, we performed immunofluorescence for CD31 and CD34. Staining for both markers was considerably increased in the bladder of UPK II-SV40 mice when compared with controls (Fig. 2, *A*–*D*). Tumor growth was associated with the development of a prom-

inent vasculature, as shown by a statistically significant increase in the CD31 area ($p = 0.017$) (Fig. 2*G*). To evaluate the maturation status of carcinoma-associated bladder vessels, we double-labeled the bladder for CD31 and NG2, a pericyte marker (Fig. 2, *E* and *F*). Pericyte coverage of vessels was similar in both groups, thus suggesting a normal maturation and function of bladder tumor-associated vasculature in this stage (Fig. 2*H*). Differences in CD31 or NG2 staining (corrected by bladder area) were not observed between males and females.

To provide further evidence of a pro-angiogenic phenotype and to explore the potential mechanism/s of vessel proliferation, Western blot of VEGF was performed using SV40 as a control for the presence of transformed urothelium. The analysis of Western blot revealed higher VEGF levels in UPK II-SV40 (+) mice (Fig. 3*A*). VEGF expression in SV40 urothelial tumors, as evaluated by immunofluorescence, was detected in stroma (Fig. 3, *B*–*G*) but was stronger in the urothelium, where it co-localized with UPK II (Fig. 3, *H*–*M*).

Because hypoxia-related pathways have a role in the generation of a tumor-associated angiogenic phenotype, hypoxia was next assessed in bladder tissues. When compared with control, UPK II-SV40 mice exhibited a higher level of hypoxia as evaluated by Hypoxyprobe labeling (Fig. 4, *A* and *B*). HIF-1α participates in angiogenesis, and it is expressed in human CIS (16, 22). We found an intense expression of HIF-1α both in the transformed urothelium and in the tumor stroma (Fig. 4, *C* and *D*), thus highlighting the participation of the hypoxia response pathway in VEGF production and neoplastic progression of bladder CIS. Staining for Glut-1, a glucose transporter whose up-regulation is usually dependent on HIF-1α (23), was also increased in bladder tumoral epithelium when compared with normal urothelium and with tumor stroma (supplemental Fig. 1, *A*–*D*).

Analysis of the expression of angiogenic growth factors and hypoxia markers, as evaluated by real time RT-PCR, showed an increase in VEGF and HIF-1β and down-regulation of thrombospondin-1 (TSP-1), a well known inhibitor of angiogenesis (19) (Fig. 4*E*). We did not find any difference between females and males in the expression of VEGF, HIF-1α, or TSP-1 (supplemental Table 3).

Bladder Carcinoma in Situ Is Associated with Modulation of Angiogenesis-related MicroRNA—Dysregulation in the expression of miRs, a group of small non-coding molecules of RNA with an important role in post-transcriptional gene regulation, is a frequent phenomenon in cancer (24). Thus, we next sought to identify modifications in the profile of miRs related to the regulation of angiogenesis (25), such as the miR-17-92 cluster (26). Whole bladder from UPK II-SV40 mice revealed an increase in the expression of miR-18a and miR-19a, which are considered responsible for pro-angiogenic effects (27), whereas miR-17/20 and miR-92a were unchanged (Fig. 5*A*). These results, taken together with TSP-1 down-regulation (Fig. 4*E*), are consistent with a pro-angiogenic effect of miR-17-92 in this model. Additionally, miR-107, another angiogenesis-related miR whose expression is thought to be dependent on p53 status (28), was significantly decreased in bladder carcinoma *in situ* when compared with normal bladder (Fig. 5*B*). A similar pattern of angiogenesis-related miR was found in both males and
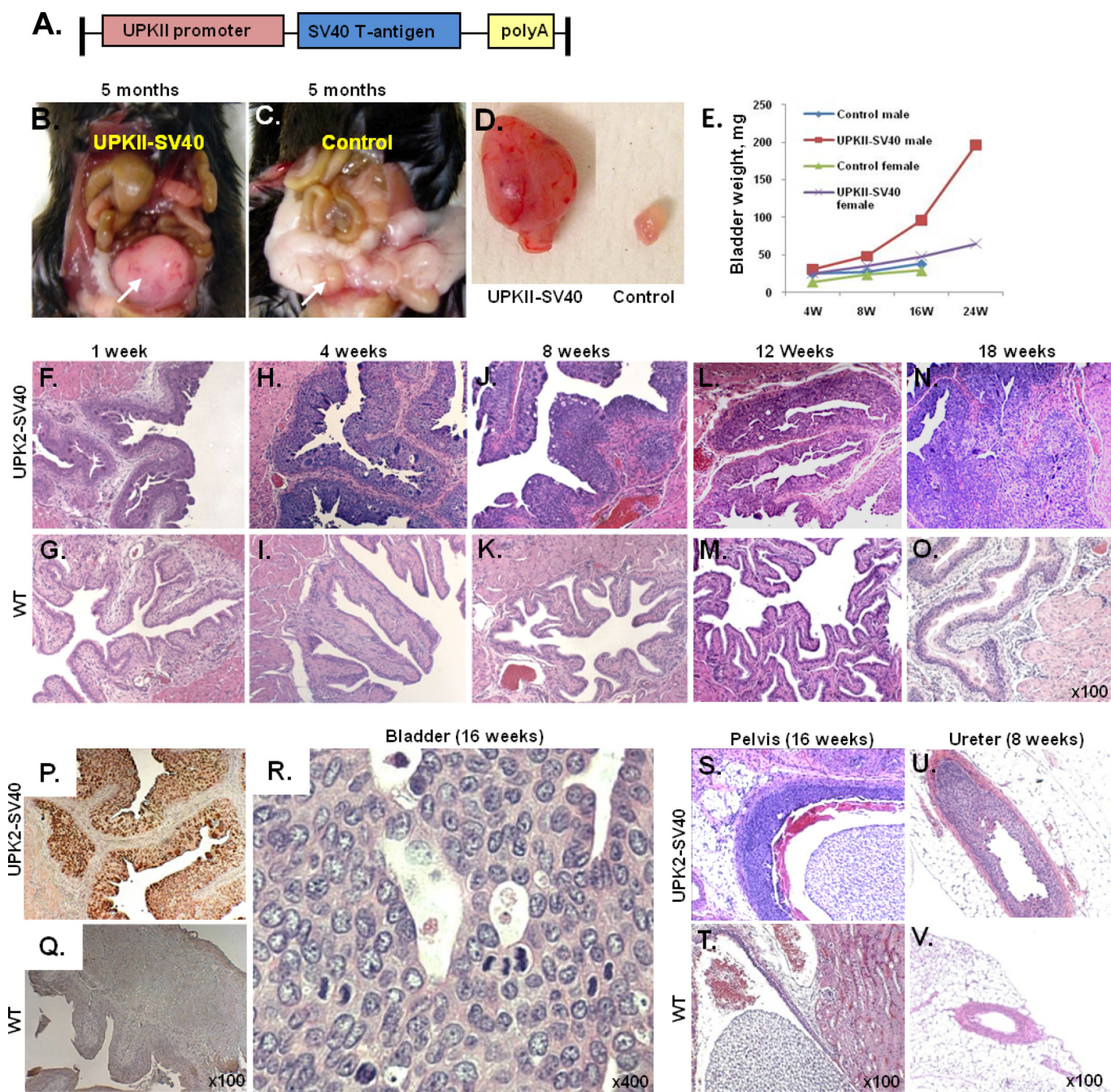
FIGURE 1. **Urothelial carcinoma *in situ* in UPK II-SV40 mice.** Transgenic mice expressing the SV40 T antigen under the control of urothelium-specific UPK II promoter spontaneously developed urothelial carcinoma *in situ*. *A*, chimeric gene consisting in the UPK II promoter, the SV40 T antigen, and a polyadenylation signal. *B–D*, macroscopic aspect of a tumor involving the whole bladder (*white arrow*) in a 5-month-old UPK II-SV40 mouse (*B*) when compared with normal bladder in a wild-type (WT) littermate (*C, white arrow*). *E*, evolution of bladder weight (in mg) in transgenic and WT mice, significantly increased in males. *F–O*, bladder urothelial CIS was evident since 1 week of age and grew progressively without muscle invasion or metastasis. *P* and *Q*, immunohistochemistry for SV40 antigen showing the urothelium-specific expression of SV40 in UPK II-SV40 mice. *R*, high-power H&E-stained sections showing an area of urothelial CIS with large and pleomorphic nuclei and loss of cell polarity. *S–V*, CIS in the renal pelvis (*S* and *T*) and ureter (*U* and *V*) of UPK II-SV40 mice when compared with normal urothelium in littermate controls.

females, although there was a trend toward increased pro-angiogenic microRNAs, such as miR-18a, miR-19, and miR-20a in the females (supplemental Table 3).

Because expression of Dicer and Drosha, two enzymes participating in miR processing, may be up-regulated in the setting of increased angiogenesis (29–31), we next analyzed their expression in bladder CIS. As shown in Fig. 5*C*, both of them exhibit significant increase in expression, consistent

with their potential role in the generation of a pro-angiogenic profile.

Uncoupling of Pro-invasive and Pro-angiogenic MicroRNA Profiles in UPK II-SV40 Urothelial Carcinoma in Situ—To determine whether differences in miR regulation might explain the uncoupling of invasion and angiogenesis in UPK II-SV40 bladder CIS, we analyzed the expression of other miRs previously reported as important for the progression or invasion of
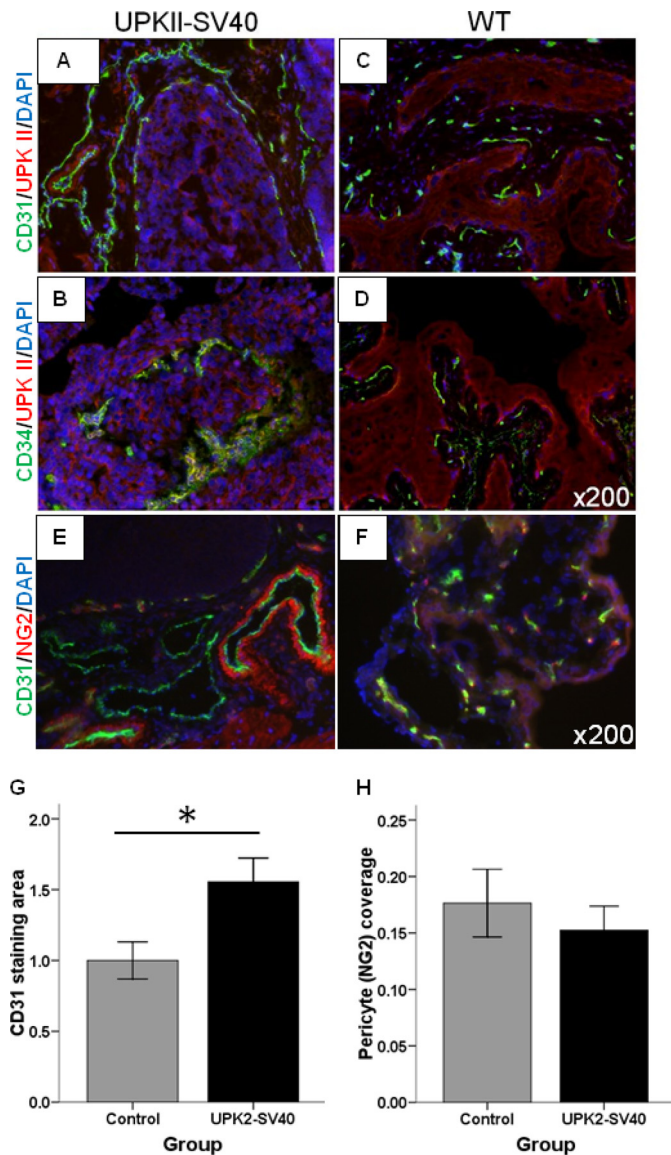
FIGURE 2. **Angiogenesis in UPK II-SV40 induced bladder carcinoma *in situ*.** Angiogenesis was evaluated in UPK II-SV40 bladder after immunofluorescence labeling of frozen sections with CD31 or CD34 (*green*) and UPK II (*red*); the nuclei were stained with DAPI (*blue*). Representative microscopic images are shown (original magnification of 200×). *A–D*, increased vessels in SV40-derived bladder carcinoma *in situ* as shown by CD31 (*A* and *C*) and CD34 (*B* and *D*) immunofluorescence. *E* and *F*, immunofluorescence of frozen bladder samples from UPK II-SV40 and control mice showed a similar pericyte coverage (labeling for NG2, *red*) of tumor-associated vessels (labeling for CD31, *green*). *G*, quantification of CD31 immunofluorescence area, related to bladder area and normalized to control values, showed a statistically significant increase of vasculature in bladder from UPK II-SV40. *, $p = 0.017$. *H*, pericyte coverage was quantified as the proportion of CD31+ vessels showing perivascular NG2 staining and was similar for both groups (0.17 in controls *versus* 0.15 in tumors; $p = 0.511$), thus reflecting a normal maturation of peritumoral vasculature in this stage of tumor development.
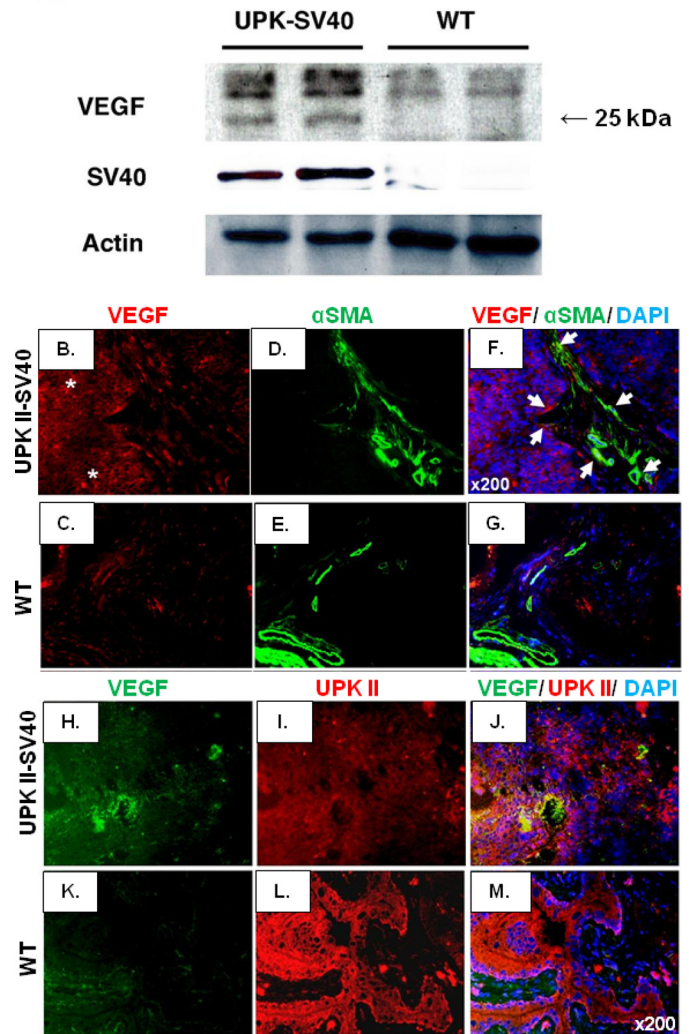

FIGURE 3. **VEGF in UPK II-SV40 bladder carcinoma.** *A*, total protein lysates from whole bladder were analyzed by Western blot for VEGF showing an increased expression of the main pro-angiogenic factor in UPK II-SV40 carcinoma *in situ*; expression of SV40 was used as a control for the presence of transformed urothelium proteins in the sample. *B–G*, the expression of VEGF was assessed by immunofluorescence for VEGF (*red*) and α-smooth muscle actin (α-SMA) (*green*), and nuclei were stained with DAPI (*blue*). Representative images (original magnification, 200×) are displayed, showing an increase in VEGF staining in UPK II-SV40 bladder carcinomas (*asterisks*) in comparison with control individuals. Although VEGF was occasionally co-localized (*white arrows*) with the fibroblast marker α-smooth muscle actin (*B–G*), double immunofluorescence for VEGF (*green*) and UPK II (*red*) showed that VEGF was mainly expressed by urothelial cells as demonstrated by its wider co-localization with uroplakin-II (*H–M*).

urothelial bladder cancer: miR-21 (32), miR-205 (32, 33), miR-34a (34), miR-222 (35), miR-129 (36), miR-200c (37), and miR-145 (36, 38, 39). As shown in Fig. 5*D*, their relative expression in bladder carcinoma *in situ* did not significantly change when compared with the normal bladder. Only miR-145 expression, related to urothelial transformation *versus* muscle invasion (38, 39), was down-regulated in UPK II-SV40 CIS. miR-21:miR-205

ratio, which has been recently reported as a sensitive marker of bladder tumor invasion, was unaltered (32).

Specific Loss of p53 in the Bladder Uroepithelium Does Not Result in Bladder Carcinoma or Acquisition of a Pro-angiogenic Phenotype—p53 allelic loss or mutations usually coexist in SV40 T-induced carcinomas and high-grade human urothelial tumors and are associated with poor prognosis. Because the precise cellular origin of bladder carcinomas is still unclear, a mouse model in which p53 deletion involves all layers of the urothelium was generated. In the UPK II-Cre;p53 f/f mouse model (Fig. 6*A*), deletion of p53 in the urothelium was not associated with formation of bladder carcinomas or other
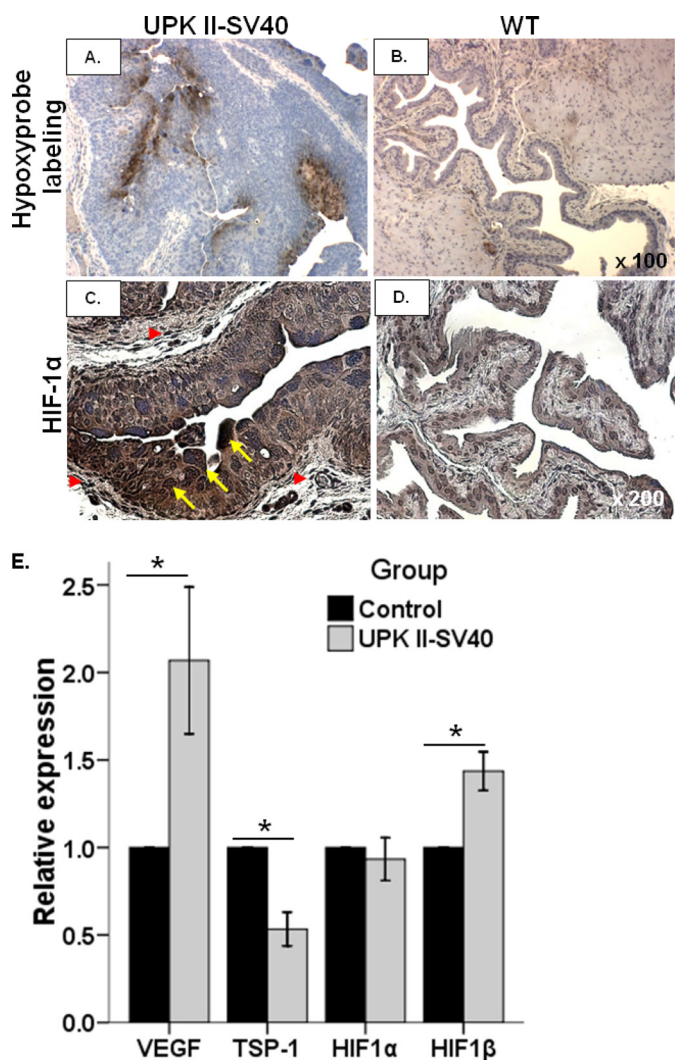
FIGURE 4. **Hypoxia and HIF-1α in UPK II-SV40 bladder carcinoma *in situ*.** *A* and *B*, hypoxia was evaluated in paraffin-embedded formalin-fixed bladder tissues obtained from UPK II-SV40 and control mice previously injected with pimonidazole (Hypoxyprobe™-1). Representative images (original magnification 100×) show that intense immunostaining for Hypoxyprobe in bladder was limited to the urothelium in carcinoma *in situ* of UPK II-SV40 mice (*A*), whereas only scarce areas of hypoxia were detected in stroma of WT mice (*B*). *C* and *D*, strong expression of HIF-1α, as shown by immunohistochemistry, was also present in the transformed urothelial cells (*C*), with a nuclear location (*yellow arrows*), but not in normal urothelium from WT mice (*D*); some peritumoral stromal areas also exhibited accumulation of HIF-1α (*red arrowheads*) (original magnification, 200×). *E*, real time RT-PCR analysis of bladder samples from UPK II-SV40 mice and controls showed a statistically significant increased expression of VEGF and HIF-1β, whereas TSP-1 was significantly down-regulated. *, $p \leq 0.02$.

FIGURE 5. **MicroRNA regulation of angiogenesis and invasion in UPK II-SV40 bladder carcinoma *in situ*.** Analysis of microRNA expression in bladder tissues was performed after stem-loop cDNA synthesis and real time RT-PCR. RNU6B was used as housekeeping gene, and the control group was the reference for quantification of relative expression. All experiments were done by triplicate, and samples from 4–5 mice were analyzed in each group. *A*, analysis of miR corresponding to cluster 17-92 showed a significantly increased expression of miR-18a (*, $p = 0.03$) and mir-19a (*, $p = 0.03$) without up-regulation of miR-20, miR-17, or miR-92a. *B*, a significant decrease in expression of miR-107 ($p = 0.04$). *C*, significant up-regulation of the RNA processing enzymes Dicer (*, $p < 0.01$) and Drosha (*, $p = 0.02$), the two main miR processing enzymes, was shown by real time RT-PCR. *D*, real time RT-PCR analysis of miR potentially related to bladder cancer progression to invasive disease did not show any statistically significant difference, except for miR-145 (*, $p = 0.02$), which was down-regulated in UPK II-SV40 bladder samples, probably reflecting urothelial transformation.

morphological alterations (Fig. 6, *B–E*). Immunolabeling confirmed the lack of p53 expression in all cell layers of urothelium (Fig. 6, *G–H*).

Further confirmation of urothelium-restricted expression of the Cre was obtained using reporter mice generated after breeding of UPK-II-Cre with Rosa-R26R-YFP floxed mice (supplemental Fig. 2*A*). When compared with control mice, YFP expression was specifically detected in the urothelial cells of bladder (supplemental Fig. 2, *B* and *C*) and ureter (supplemental Fig. 2, *D* and *E*) of UPK II-Cre; Rosa-Stop-YFP$^{+/+}$ mice. Cre-mediated excision of the STOP cassette was also demonstrated by PCR for the recombinant YFP in the bladder DNA
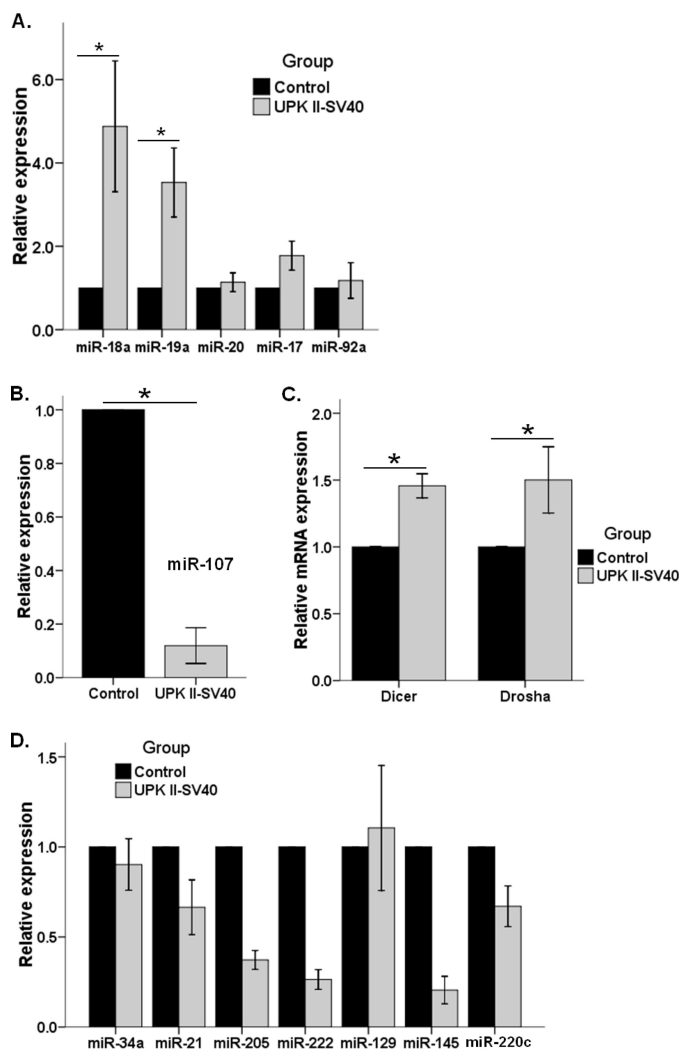
from UPK II-Cre; Rosa-Stop-YFP$^{+/+}$ mice (supplemental Fig. 2*F*).

To determine whether the pro-angiogenic profile observed in the UPK II-SV40 mice was related to p53 deletion, we examined the vasculature of bladders from UPK II-Cre;p53 f/f mice. As shown in Fig. 7, *A* and *B*, increased vascularization was not observed in UPK II-Cre;p53 f/f mice, when evaluated using immunofluorescence for CD31 (Fig. 7*C*). Pericyte coverage of blood vessels was also similar in both groups. We did not observe any difference in hypoxia response as evaluated using HIF-1α staining (Fig. 7, *D* and *E*) and VEGF staining (data not shown) Finally, analysis of the expression of angiogenic factors
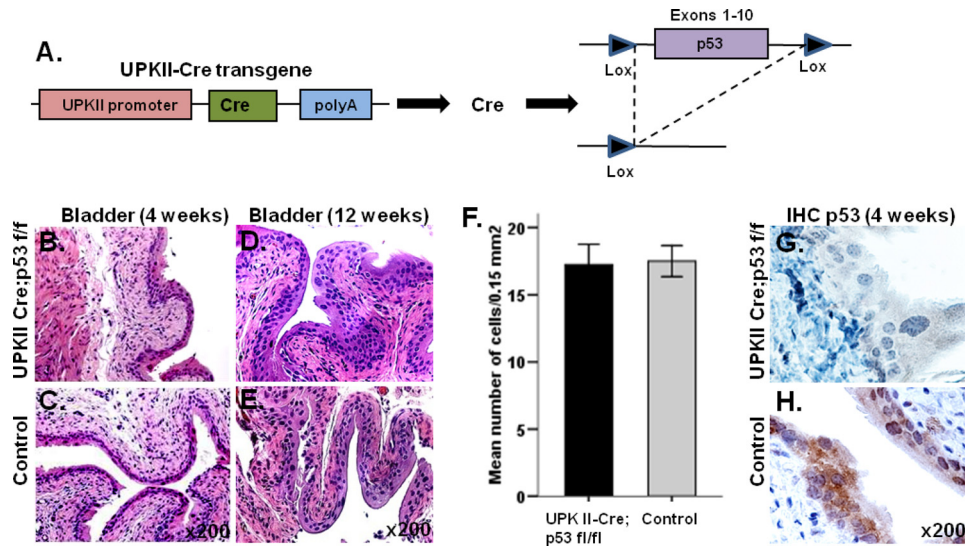
FIGURE 6. **Absence of urothelium defects in the UPK II-Cre;p53 mice.** *A,* urothelial-restricted Cre-mediated deletion of p53 (exons 1–10). *B–E,* H&E-stained cross-sections of 4-week-old (*B* and *C*) and 12-week-old (*D* and *E*) bladder showed a normal urothelium in both UPK II-Cre;p53 and WT individuals. *F,* no differences in urothelium cell count between both groups ($n = 6$) were observed ($p = 0.89$); *bars* indicate S.E. *G* and *H,* staining for p53 confirmed deletion in UPK II-Cre;p53 mice. *IHC,* immunohistochemistry.

and hypoxia mediators revealed insignificant differences between controls and UPK II-Cre;p53 f/f mice (Fig. 7*F*). In particular, TSP-1 levels were not decreased in UPK II-Cre;p53 f/f urothelium. Taken together, these data demonstrate that isolated p53 deletion is not sufficient in inducing an angiogenic phenotype in the urothelium.

Finally, we also analyzed the microRNA profile of bladders from UPK II-Cre;p53 f/f and found that neither miR-107 nor the miR-17-92 cluster was up-regulated. Invasion-related miR (miR-21, miR-205, miR-222, and miR-34a) also revealed similar expression levels in both groups (Fig. 7, *G* and *H*). These results differ from those observed in the UPK II-SV40 model and suggest that the development of an angiogenesis-related miR profile is not dependent on just p53 inactivation alone. Thus, additional oncogenic events, besides p53 deletion, are necessary for generating both a pro-angiogenic profile and development of urothelial carcinoma *in situ.*

DISCUSSION

Angiogenesis is a key process in the growth and malignant progression of human cancer. The tightly regulated physiological balance between pro- and anti-angiogenic signals is influenced by cancer cells and the tumor stromal cells, leading to the development of a vascular network that is able to support the growth and invasion of the tumor (40). Although much has been unraveled in the last several years about the mechanisms by which tumor angiogenesis increases and participates in cancer progression, the role of microRNA in its regulation is only beginning to be understood. MicroRNAs are small non-coding molecules of RNA important in post-transcriptional gene regulation via either inhibition of translation or degradation of mRNA (41). After a complex processing step, mature single strand miRs are able to target a wide range of partially complementary specific sequences, thus participating in the regulation of many biological functions (42). As it has been recently shown, modifications in the miR expression profile can be observed in most human diseases, and specifically, dysregulation of miR is a frequent occurrence in cancer (24). miRs are key steps of cancer progression including angiogenesis (25), invasion (43), and metastasis (37, 44). In the setting of urothelial bladder cancer, altered regulation in a number of miRs and specific miR patterns have also been reported for urothelial carcinogenesis (38, 39), high histological grade (34), invasive phenotype (32, 33), and metastatic phenotype (35, 45).

Also, the significance of angiogenesis for progression of superficial bladder carcinoma, and specifically, carcinoma *in situ* is yet unexplored. In clinical studies, an increased angiogenesis seems to be related to superficial bladder carcinoma of histological grade, but its prognostic relevance for recurrence or progression to muscle-invasive disease, which is a significant concern in the clinical management of patients with bladder CIS presentation, remains unclear (10–12). To provide further insights into the functional role of angiogenesis in urothelial carcinoma *in situ,* we generated transgenic mice in which the urothelium-specific expression of SV40 large T antigen leads to malignant transformation and induces bladder carcinoma *in situ.* In this model, we were able to demonstrate development of bladder carcinoma *in situ* and increased angiogenesis, but progression to invasive disease was not identified. Therefore, our results suggest that inactivation of p53 and pRb, an increase in angiogenesis, and angiogenesis-related microRNA pattern are not sufficient for emergence of invasive bladder carcinoma.

The inactivation of p53, a consequence of SV40 T antigen expression (3) and a speculated fundamental step in the origin of urothelial carcinoma *in situ* (4), has been linked to a pro-angiogenic response in bladder cancer (46, 47). In contrary, our experiments suggest that specific loss of p53 in the bladder urothelium is not sufficient to induce angiogenesis or bladder cancer.

In the UPK II-SV40 model of urothelial CIS, a higher VEGF expression was observed, and as shown by co-localization with
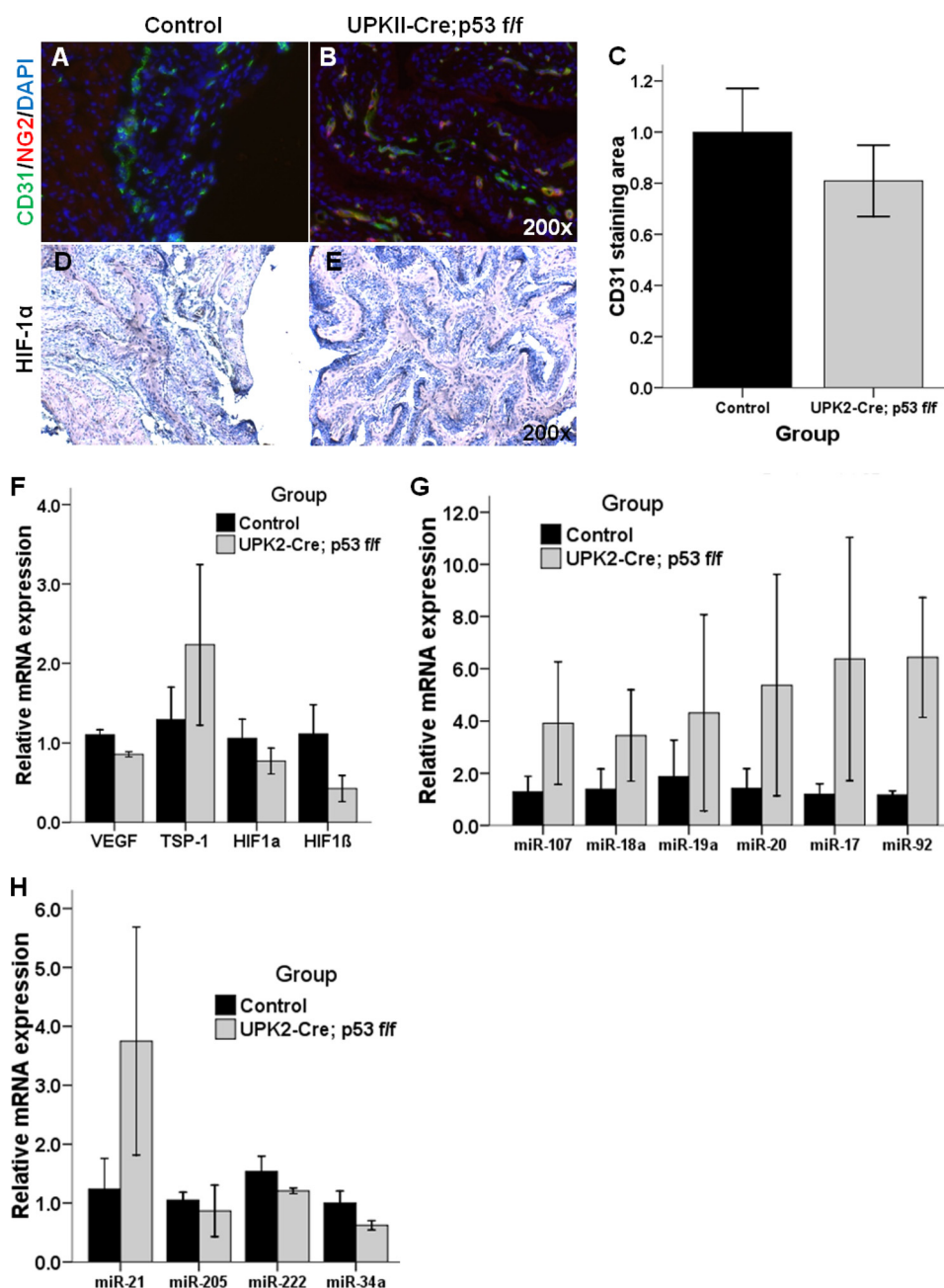
FIGURE 7. **Angiogenic factors in bladders of UPK II-Cre;p53 f/f.** Vascularization was evaluated in UPK II-Cre;p53 f/f bladder with immunofluorescence of frozen sections for CD31 (*green*) and NG2 (*red*); the nuclei were stained with DAPI (*blue*). Representative microscopic images are shown (original magnification of 200×). *A* and *B*, no increased vessels or changes in pericyte coverage were observed in UPK II-Cre;p53 f/f when compared with controls. *C*, quantification of CD31 immunofluorescence area, related to bladder area and normalized to control values, showed similar values in both groups ($p = 0.72$). *D* and *E*, immunohistochemistry for HIF-1α in bladder urothelial cells was also similar in controls and UPK II-Cre;p53 f/f mice. *F*, real time RT-PCR analysis of bladder samples from UPK II-Cre;p53 f/f mice and controls did not show statistically significant differences in expression of VEGF, TSP-1, HIF-1α, and HIF-1β, although decrease in VEGF and HIF-1β in the UPK II-Cre;p53 f/f bladder bordered on significance ($p = 0.08$). *G* and *H*, analysis of microRNA expression in bladder tissues was performed using the control group as the reference for quantification of relative expression. All experiments were done by triplicate, and samples from three mice were analyzed in each group. *G*, in UPK II-Cre;p53 f/f bladder, we found an increase in the expression of both miR-107 and members of the cluster miR-17-92, which was not statistically significant ($p > 0.40$ for all of them, except for miR-17 and miR-92, $p = 0.12$). *H*, analysis of miR potentially related to bladder cancer invasion (miR-21, miR-205, miR-222, and miR-34a) did not show any statistically significant differences between controls and UPK II-Cre;p53 f/f.

UPK II, it presents in the transformed epithelium (20). Additionally, bladder CIS also exhibits significant down-regulation of TSP-1 expression, previously reported as critical in the acquisition of angiogenic phenotype in an androgenic-dependent model of bladder carcinoma (19). In this model, a general pattern of increased vascularization and pro-angiogenic signals was associated with hypoxia and HIF-1α and HIF-1β up-regu-

lation (16, 22). Despite the higher rate of tumor growth in males, we did not detect a difference in the angiogenic factors between males and females, suggesting that angiogenic activation is not merely dependent on tumor size.

Our results suggest that pro-angiogenic profile may be partially explained by differences in microRNA regulation. Previous reports have shown that the miR-17-92 cluster (also known

as OncomiR-1), which includes miR-17, miR-18, miR-19a, miR-20a, and miR-92, may promote tumor angiogenesis by inhibition of TSP-1 and other factors (26), although some of its members, such as miR-17, might also exhibit anti-angiogenic activity under certain conditions (27). The increased expression of pro-angiogenic miR-18a and miR-19a in UPK2-SV40 mice, taken together with normal levels of miR-17/20, suggests a potential pro-angiogenic role for miR-17-92 in bladder CIS.

Recent data show that the p53-dependent miR-107 up-regulation is able to inhibit HIF-1β and hypoxic signaling in cancer cells, consequently limiting tumor angiogenesis (27). SV40 large T antigen functionally inactivates p53. Therefore, we hypothesized that in UPK II-SV40 bladder tumors, mir-107 may be down-regulated. This possibility was supported by observing a striking decrease in miR-107 levels in bladder CIS, which could also explain in part the enhanced hypoxic response observed in our model. Additionally, regulation of miR expression in general is also dependent on the activity of two miR processing enzymes: Dicer and Drosha. Down-regulation or loss of Dicer impairs angiogenesis *in vitro* (29, 30) and *in vivo* (31) via up-regulation of TSP-1. We observed exactly the reverse pattern in the UPK II-SV40 bladder CIS. Moreover, we did not observe up-regulation of angiogenic factors and angiogenesis-related miRs in the UPK II-Cre;p53 f/f mice. miR-107 levels were not altered. These results question the contribution of isolated p53 deletion in the urothelium for the emergence of angiogenesis phenotype.

A predominant feature of our model of urothelial CIS was the absence of invasion, even in large tumors. Several clinical studies and experimental studies using *in vitro* and *in vivo* models have identified a number of miRs as important for progression and invasion associated with urothelial cancer. Some of them, such as miR-145 (36, 38, 39) or miR-34a (34, 48), are characteristically down-regulated in bladder carcinomas and may act as tumor suppressors, but their relation to invasive disease is unclear. Others, like miR-21 (32, 34, 36) or miR-222 (35), can be up-regulated in carcinomas and are frequently regarded as markers for invasive cancer. Down-regulation or silencing of miR-205 has been proposed as a predictor of invasive urothelial tumors (32, 33, 36). The ratio miR-21:miR-205 was recently proposed as a marker of muscle-invasive disease (32). In our model, no significant changes in the expression levels of those invasion-related miRs or in the miR-21:miR-205 ratio were observed. Similarly, miR-129, whose up-regulation is related to progression, poor prognosis, and T2–4 stages (36), was not significantly increased in UPK II-SV40 bladder CIS. Finally, we did not find changes in miR-200c, down-regulation of which in bladder cancer is associated with epithelial to mesenchymal transition (33, 49), a process by which cancer cells acquire invasive or metastatic capabilities (50).

In conclusion, our UPK II-SV40 model of bladder CIS provides some insights on the natural history of this neoplasia. Although we observed a rapid emergence of tumors in the bladder, we did not find an evolution to muscle-invasive tumors or metastasis, which were reported as infrequent events in previous publications (3, 4) and may be related to the accumulation of other mutations or tumor suppressor inactivations (51). In this particular model, the induction of a strong angiogenic phenotype was not sufficient for the development of muscle invasion or metastasis. Analysis of miR expression exhibited a pattern of change consistent with pro-angiogenic phenotype, but miRs related to invasion were essentially unmodified in our UPK II-SV40 urothelial tumors. These data should be considered in the context of the controversial reports for the role of angiogenesis markers in predicting recurrence or invasion in clinical studies with superficial bladder carcinomas (11–13, 52).

REFERENCES

1. Jemal, A., Siegel, R., Ward, E., Hao, Y., Xu, J., and Thun, M. J. (2009) *CA Cancer J. Clin.* **59,** 225–249
2. Pasin, E., Josephson, D. Y., Mitra, A. P., Cote, R. J., and Stein, J. P. (2008) *Rev. Urol.* **10,** 31–43
3. Zhang, Z. T., Pak, J., Shapiro, E., Sun, T. T., and Wu, X. R. (1999) *Cancer Res.* **59,** 3512–3517
4. Cheng, J., Huang, H., Pak, J., Shapiro, E., Sun, T. T., Cordon-Cardo, C., Waldman, F. M., and Wu, X. R. (2003) *Cancer Res.* **63,** 179–185
5. Mo, L., Cheng, J., Lee, E. Y., Sun, T. T., and Wu, X. R. (2005) *Am. J. Physiol. Renal Physiol* **289,** F562–f568
6. He, F., Mo, L., Zheng, X. Y., Hu, C., Lepor, H., Lee, E. Y., Sun, T. T., and Wu, X. R. (2009) *Cancer Res.* **69,** 9413–9421
7. Puzio-Kuter, A. M., Castillo-Martin, M., Kinkade, C. W., Wang, X., Shen, T. H., Matos, T., Shen, M. M., Cordon-Cardo, C., and Abate-Shen, C. (2009) *Genes Dev.* **23,** 675–680
8. Gao, J., Huang, H. Y., Pak, J., Cheng, J., Zhang, Z. T., Shapiro, E., Pellicer, A., Sun, T. T., and Wu, X. R. (2004) *Oncogene* **23,** 687–696
9. Kaufman, D. S., Shipley, W. U., and Feldman, A. S. (2009) *Lancet* **374,** 239–249
10. Mitra, A. P., Datar, R. H., and Cote, R. J. (2006) *J. Clin. Oncol.* **24,** 5552–5564
11. Sağol, O., Yörükoğlu, K., Sis, B., Tuna, B., Ozer, E., Güray, M., Mungan, U., and Kirkali, Z. (2001) *Urology* **57,** 895–899
12. Stavropoulos, N. E., Bouropoulos, C., Ioachim, I. E., Michael, M., Hastazeris, K., Tsimaris, I., Kalogeras, D., Liamis, Z., Stefanaki, S., and Agnantis, N. I. (2004) *Int. Urol. Nephrol.* **36,** 163–167
13. Crew, J. P., O'Brien, T., Bicknell, R., Fuggle, S., Cranston, D., and Harris, A. L. (1999) *J. Urol.* **161,** 799–804
14. Izawa, J. I., Slaton, J. W., Kedar, D., Karashima, T., Perrotte, P., Czerniak, B., Grossman, H. B., and Dinney, C. P. (2001) *Oncol. Rep.* **8,** 9–15
15. Fauconnet, S., Bernardini, S., Lascombe, I., Boiteux, G., Clairotte, A., Monnien, F., Chabannes, E., and Bittard, H. (2009) *Oncol. Rep.* **21,** 1495–1504
16. Ioachim, E., Michael, M., Salmas, M., Michael, M. M., Stavropoulos, N. E., and Malamou-Mitsi, V. (2006) *Urol. Int.* **77,** 255–263
17. Srinivas, S., Watanabe, T., Lin, C. S., William, C. M., Tanabe, Y., Jessell, T. M., and Costantini, F. (2001) *BMC Dev. Biol.* **1,** 4
18. Chen, C., Ridzon, D. A., Broomer, A. J., Zhou, Z., Lee, D. H., Nguyen, J. T., Barbisin, M., Xu, N. L., Mahuvakar, V. R., Andersen, M. R., Lao, K. Q., Livak, K. J., and Guegler, K. J. (2005) *Nucleic Acids Res.* **33,** e179
19. Johnson, A. M., O'Connell, M. J., Miyamoto, H., Huang, J., Yao, J. L., Messing, E. M., and Reeder, J. E. (2008) *BMC Urol.* **8,** 7
20. Epstein, J. I., Amin, M. B., Reuter, V. R., and Mostofi, F. K. (1998) *Am. J. Surg. Pathol.* **22,** 1435–1448
21. Catalano, A., Romano, M., Martinotti, S., and Procopio, A. (2002) *Oncogene* **21,** 2896–2900
22. Jones, A., Fujiyama, C., Blanche, C., Moore, J. W., Fuggle, S., Cranston, D., Bicknell, R., and Harris, A. L. (2001) *Clin Cancer Res.* **7,** 1263–1272
23. Palit, V., Phillips, R. M., Puri, R., Shah, T., and Bibby, M. C. (2005) *Oncol. Rep.* **14,** 909–913
24. Iorio, M. V., and Croce, C. M. (2009) *J. Clin. Oncol.* **27,** 5848–5856
25. Wang, S., and Olson, E. N. (2009) *Curr. Opin. Genet. Dev.* **19,** 205–211
26. Dews, M., Homayouni, A., Yu, D., Murphy, D., Sevignani, C., Wentzel, E.,

Furth, E. E., Lee, W. M., Enders, G. H., Mendell, J. T., and Thomas-Tik-honenko, A. (2006) *Nat. Genet.* **38,** 1060–1065

27. Doebele, C., Bonauer, A., Fischer, A., Scholz, A., Reiss, Y., Urbich, C., Hofmann, W. K., Zeiher, A. M., and Dimmeler, S. (2010) *Blood* **115,** 4944–4950

28. Yamakuchi, M., Lotterman, C. D., Bao, C., Hruban, R. H., Karim, B., Mendell, J. T., Huso, D., and Lowenstein, C. J. (2010) *Proc. Natl. Acad. Sci. U.S.A.* **107,** 6334–6339

29. Kuehbacher, A., Urbich, C., and Dimmeler, S. (2008) *Trends Pharmacol. Sci.* **29,** 12–15

30. Kuehbacher, A., Urbich, C., Zeiher, A. M., and Dimmeler, S. (2007) *Circ. Res.* **101,** 59–68

31. Suárez, Y., Fernández-Hernando, C., Yu, J., Gerber, S. A., Harrison, K. D., Pober, J. S., Iruela-Arispe, M. L., Merkenschlager, M., and Sessa, W. C. (2008) *Proc. Natl. Acad. Sci. U.S.A.* **105,** 14082–14087

32. Neely, L. A., Rieger-Christ, K. M., Neto, B. S., Eroshkin, A., Garver, J., Patel, S., Phung, N. A., McLaughlin, S., Libertino, J. A., Whitney, D., and Summerhayes, I. C. (2010) *Urol. Oncol.* **28,** 39–48

33. Wiklund, E. D., Bramsen, J. B., Hulf, T., Dyrskjøt, L., Ramanathan, R., Hansen, T. B., Villadsen, S. B., Gao, S., Ostenfeld, M. S., Borre, M., Peter, M. E., Ørntoft, T. F., Kjems, J., and Clark, S. J. (2011) *Int. J. Cancer* **128,** 1327–1334

34. Catto, J. W., Miah, S., Owen, H. C., Bryant, H., Myers, K., Dudziec, E., Larré, S., Milo, M., Rehman, I., Rosario, D. J., Di Martino, E., Knowles, M. A., Meuth, M., Harris, A. L., and Hamdy, F. C. (2009) *Cancer Res.* **69,** 8472–8481

35. Veerla, S., Lindgren, D., Kvist, A., Frigyesi, A., Staaf, J., Persson, H., Liedberg, F., Chebil, G., Gudjonsson, S., Borg, A., Månsson, W., Rovira, C., and Höglund, M. (2009) *Int. J. Cancer* **124,** 2236–2242

36. Dyrskjøt, L., Ostenfeld, M. S., Bramsen, J. B., Silahtaroglu, A. N., Lamy, P., Ramanathan, R., Fristrup, N., Jensen, J. L., Andersen, C. L., Zieger, K., Kauppinen, S., Ulhøi, B. P., Kjems, J., Borre, M., and Orntoft, T. F. (2009) *Cancer Res.* **69,** 4851–4860

37. Olson, P., Lu, J., Zhang, H., Shai, A., Chun, M. G., Wang, Y., Libutti, S. K., Nakakura, E. K., Golub, T. R., and Hanahan, D. (2009) *Genes Dev.* **23,** 2152–2165

38. Ostenfeld, M. S., Bramsen, J. B., Lamy, P., Villadsen, S. B., Fristrup, N., Sørensen, K. D., Ulhøi, B., Borre, M., Kjems, J., Dyrskjøt, L., and Orntoft, T. F. (2010) *Oncogene* **29,** 1073–1084

39. Ichimi, T., Enokida, H., Okuno, Y., Kunimoto, R., Chiyomaru, T., Kawamoto, K., Kawahara, K., Toki, K., Kawakami, K., Nishiyama, K., Tsujimoto, G., Nakagawa, M., and Seki, N. (2009) *Int. J. Cancer* **125,** 345–352

40. Folkman, J., and Kalluri, R. (2004) *Nature* **427,** 787

41. Carthew, R. W., and Sontheimer, E. J. (2009) *Cell* **136,** 642–655

42. Bartel, D. P. (2009) *Cell* **136,** 215–233

43. Li, N., Fu, H., Tie, Y., Hu, Z., Kong, W., Wu, Y., and Zheng, X. (2009) *Cancer Lett.* **275,** 44–53

44. Asangani, I. A., Rasheed, S. A., Nikolova, D. A., Leupold, J. H., Colburn, N. H., Post, S., and Allgayer, H. (2008) *Oncogene* **27,** 2128–2136

45. Baranwal, S., and Alahari, S. K. (2010) *Int. J. Cancer* **126,** 1283–1290

46. Bochner, B. H., Esrig, D., Groshen, S., Dickinson, M., Weidner, N., Nichols, P. W., Skinner, D. G., and Cote, R. J. (1997) *Clin. Cancer Res.* **3,** 1615–1622

47. Grossfeld, G. D., Ginsberg, D. A., Stein, J. P., Bochner, B. H., Esrig, D., Groshen, S., Dunn, M., Nichols, P. W., Taylor, C. R., Skinner, D. G., and Cote, R. J. (1997) *J. Natl. Cancer Ins.t* **89,** 219–227

48. Lodygin, D., Tarasov, V., Epanchintsev, A., Berking, C., Knyazeva, T., Körner, H., Knyazev, P., Diebold, J., and Hermeking, H. (2008) *Cell Cycle* **7,** 2591–2600

49. Adam, L., Zhong, M., Choi, W., Qi, W., Nicoloso, M., Arora, A., Calin, G., Wang, H., Siefker-Radtke, A., McConkey, D., Bar-Eli, M., and Dinney, C. (2009) *Clin. Cancer Res.* **15,** 5060–5072

50. Kalluri, R., and Weinberg, R. A. (2009) *J. Clin. Invest.* **119,** 1420–1428

51. Cordon-Cardo, C. (2008) *Scand. J. Urol. Nephrol.* **218,** 154–165

52. Turner, K. J., Crew, J. P., Wykoff, C. C., Watson, P. H., Poulsom, R., Pastorek, J., Ratcliffe, P. J., Cranston, D., and Harris, A. L. (2002) *Br. J. Cancer* **86,** 1276–1282